

Development of Novel Bevel-Geared 5 mm Articulating Wrist for Micro-Laparoscopy Instrument

Jongwoo Kim , *Student Member, IEEE*, Hyung-Taeg Han , *Student Member, IEEE*,
Sungchul Kang , *Member, IEEE*, and Chunwoo Kim , *Member, IEEE*

Abstract—A laparoscopic surgery can be made less invasive by utilizing slimmer tools. However, at the size scale of the microlaparoscopic instruments, it has been very challenging to incorporate a wrist mechanism for dexterous manipulation at the surgical sites. In this letter, we present a 5-mm wristed instrument for microlaparoscopy. Unlike other instruments with wrists utilizing the bending of compliant parts or tendon and pulleys, the instrument has a wrist mechanism using oblique bevel gears driven by two concentric shafts. As a result, the wrist can generate a 2-degrees-of-freedom sharp articulating motion with 1) pitch angle range of $\pm 90^\circ$ and 2) a full rotation along roll direction. Also, the wrist is scalable and easier to assemble compared to the ones using tendon and pulleys. The accuracy and the load carrying capacity of the wrist were evaluated. The wrist was able to orient tools to the commanded direction with an average error of 1.31° and manipulate up to 250 g of the load. The feasibility of the instrument was verified through pick and place experiment and peg transfer test using a teleoperated surgical robot equipped with the instrument. Using the single robot arm with the proposed wrist, it took 98.7 s on average to transfer five objects consecutively to the opposite side of the pegboard. Thus, the articulating wrist widens dexterity in tight anatomic space with the oblique gear mechanism. It is applicable to needlescopic instruments or steerable laparoscope system.

Index Terms—Mechanism design, medical robots and systems, minimally invasive surgery, surgical robotics: laparoscopy.

I. INTRODUCTION

WITH the surgical robot technology trending toward the minimally invasive surgery, many robotic systems and tools for laparoscopic surgery have been developed [1]–[4]. Researchers have studied various mechanisms for minimally invasive surgical robots such as cable-driven mechanism [5]–[9],

super elastic cable [10], [11], flexible fluidic actuator [12]–[17], smart material actuator [18]–[22], and magnet actuators [23]–[26], and the wire-guided linkage [27]. Researchers aim to develop slimmer and dexterous laparoscopic surgical instruments compared to the conventional ones. Traditionally, the multi-port laparoscopic surgery usually requires 5~10 mm incisions on four locations. When the port size decreases with the advanced surgical instruments, it minimizes access trauma, shortens hospitalization, and improves therapeutic outcome [28], [29] in various operations such as colorectal surgery [30] and hepatectomy [31]. If the diameter of the laparoscopic instruments is below 3 mm, the invasiveness of the instrument port approaches that of a hypodermic needle and leaves almost no scar. Micro-laparoscopic surgery, a multi-port laparoscopic surgery using slimmer (<5 mm diameter) instruments, is not only less invasive but also fewer complications [32].

Micro-laparoscopic instruments with a diameter as small as 2mm [33] are commercially available. However, most of the instruments lack a wrist for dexterous manipulation of its end effectors, as it is very challenging to integrate one at the size scale of the micro-laparoscopic instruments. At the size scale of 5 mm or less in diameter, researchers often utilize the cable-driven rolling joint mechanism for manipulation, including da Vinci surgical system [7], [34]. Additionally, few ‘wristed’ micro-laparoscopic instruments with diameter below 5 mm have been demonstrated in product level and research level [35]–[37]. Most of the wrist used in these micro-laparoscopic instruments take the form of continuum robots [38]–[41] that generates motion through the deformations of a bending section.

For dexterous manipulation inside tight anatomic spaces, the wrist should 1) be able to generate a sharp articulating motion about a pivot point and 2) have minimal motion envelop. In view of these two requirements, the ‘articulating’ wrist is preferable to the ‘bending’ wrist in terms of space savings. Due to the length of a bending section and its finite curvature, the bending wrist cannot make a sharp turn and as a result, it requires larger motion envelop to achieve the same end-effector orientation. In particular, as illustrated in Fig. 1, the bending wrist’s unit vector of the tool direction, \vec{V}_{tip} , is located at a distance from the pivot point compared to the one of the articulating wrist. It means that the bending wrist needs more space to orient the tip inside the body. On the other hand, the articulating wrist can make a sharp turn at the pivot point so it has a smaller motion envelope.

Such an ‘articulating wrist’ requires a mechanism for transmitting the actuator motion along the long instrument shaft

Manuscript received February 24, 2019; accepted June 18, 2019. Date of publication July 15, 2019; date of current version July 26, 2019. This letter was recommended for publication by Associate Editor S. Zuo and Editor P. Valdastri upon evaluation of the reviewers’ comments. This work was supported by the Korea Institute of Science and Technology Institutional Program under Grant 2E28230. (*Corresponding author: Chunwoo Kim.*)

J. Kim is with the Biorobotics Laboratory/Soft Robotics Research Center Department of Mechanical and Aerospace Engineering, Seoul National University, Seoul 08826, South Korea, and also with the Center for Medical Robotics, Korea Institute of Science and Technology, Seoul 02792, South Korea (e-mail: kimjongwoo1988@gmail.com).

H.-T. Han and C. Kim are with the Center for Medical Robotics, Korea Institute of Science and Technology, Seoul 02792, South Korea (e-mail: 118022@kist.re.kr; cwkim@kist.re.kr).

S. Kang is with the Robot Center, Samsung Research, Seoul 06765, South Korea (e-mail: kasch804@gmail.com).

This letter has supplementary downloadable material available at <http://ieeexplore.ieee.org>, provided by the authors.

Digital Object Identifier 10.1109/LRA.2019.2928779

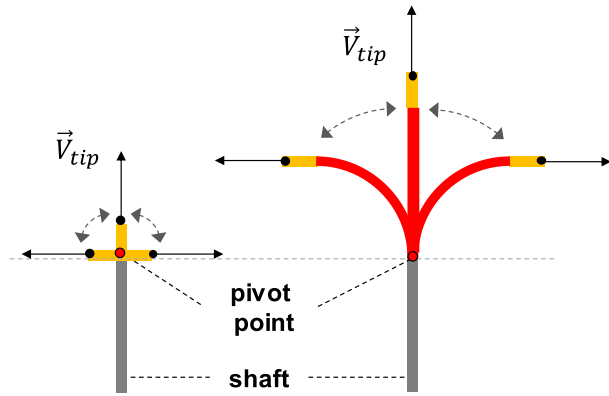


Fig. 1. The comparison of the motion envelop between articulating wrists (left) and bending wrists (right). The black arrow indicates the unit vector of the tool (yellow bar) direction at given configuration. To turn the tool by ± 90 degrees, the articulating wrists (left) rotates about the pivot point (red dot). On the other hand, the bending wrists (right) must have a bending section with some length (red bar). Thus, the articulating wrists have sharper turn and smaller motion envelop compared to the bending wrists.

and converting the transmitted actuation into a rotation about fixed axes perpendicular to the axis of the instrument shaft. Traditional laparoscopic instruments with an articulating wrist use tendon and pulley. Tendon and pulley mechanism requires an antagonistic pair of tendon and a pin joint to mount the pulley [42]. However, machining and assembling pulleys, the strength of pin joints, and tensioning and routing the tendons become challenging with the decreasing diameter of the instrument. Tendon pulley mechanisms are difficult to be scaled down to the sizes of micro-laparoscopic instruments and special manufacturing technology had to be developed to build 3 mm articulating wrist using tendon and pulley [35]. Thus, it has been very challenging to integrate an articulating wrist to micro-laparoscopic instruments due to its scalability.

In order to make laparoscopic instruments slimmer yet dexterous, a new wrist mechanism needs to be developed to transmit and convert the actuator motion from the proximal end of the tool into ‘the articulating motion’ at the distal end. Also, this wrist mechanism should be simple and scalable to the sizes of micro-laparoscopic tools in terms of manufacturing and assembly and provide sharp articulating motion. In this research, we present 5 mm micro-laparoscopic instrument equipped with a novel wrist mechanism capable of sharp articulation. Unlike other instruments with wrist mechanisms based on the bending of compliant parts, the instrument has the wrist mechanism using oblique bevel gear that can generate a sharp articulating motion with a pitch angle range of ± 90 degrees and full rotation along roll direction. The 2-DoF articulated wrist with rolling and pitch ability also have smaller motion envelop compared to other mechanisms.

In addition, the proposed wrist is based on a solid gear mechanism rather than the deflection of compliant material, thus improving the resolution and precision of motion control. M. Mitsuishi *et al.* have researched the mechanism with multiple sets of orthogonal bevel gears to develop hand-held multi-DoF forceps for laparoscopic surgery [43], [44]. The proposed wrist

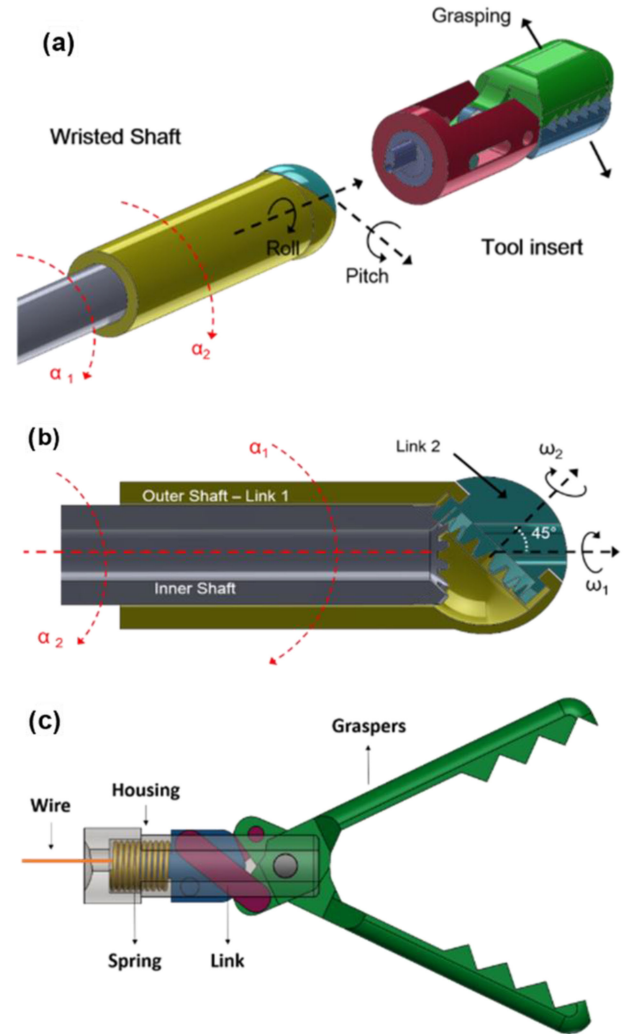


Fig. 2. (a) The structure of the presented 5 mm micro-laparoscopic instruments, (b) the cross section of the wrist mechanism, (c) the cross section of the spring-loaded grasper.

also utilizes bevel gear set, but the axes between the gears have oblique angles to have a larger diameter of the output gear while satisfying the geometric constraint of the whole structure. The larger diameter of the gear can facilitate the machining process and increase the maximum torque delivered by the mechanism. The proposed wrist is controlled by rotating two concentric shafts, making it easier to assemble compared to tendon pulley. We evaluated the performance of the wrist by measuring the accuracy of tip direction control and static and dynamic load capability. Furthermore, the feasibility of a robotic micro-laparoscopic instrument with the articulating wrist was verified by the pick and placement test and peg transfer test using the teleoperated master/slave surgical robot system.

II. DESIGN OF THE INSTRUMENT

The presented instrument consists of a shaft with a wrist and a grasper attached to it as shown in Fig. 2(a). Two degrees of freedom (DoF) wrist mechanism using oblique bevel gears orients

the grasper. Grasper has spring loaded slider crank mechanism to open and close it in any orientations. Two main considerations in the design of the instrument were 1) generation of sharp articulating motion, and 2) scalability to 5 mm shaft diameter, both in terms of manufacturing and assembly.

A. Wrist Mechanism

In laparoscopic instruments, due to its long and slim structure, actuators are located at the proximal end and the actuations must be transmitted along the instrument shaft to a wrist and an end effector at the distal end. Most of the wristed laparoscopic instruments use tendons for this transmission. However, due to routing and tensioning, assembling tendons becomes more difficult with increasing number of actuations and decreasing sizes.

In the presented instrument, actuations for the wrist mechanism are transmitted by rotation of two concentric shafts, which lead to a simple and scalable structure. Rotation about the major axis is a natural and effective method of transmitting motion from one end to the other end of a long slender shaft. The concentric arrangement of the shafts is easy to assemble and scalable since the metal tubes with small diameters are readily available. Furthermore, the concentric arrangement leaves space in the central lumen that can be utilized to deliver signal lines or actuating tendons for the tool that will be attached to the wrist.

Articulating motion about a pivot point like that of the human wrist can be generated by combining rotation about two non-parallel axes intersecting at a common point. Therefore, to create articulating wrist motion from two aligned rotations transmitted by the concentric shafts, the direction of one of the concentric rotation needs to be changed. For this rotation direction conversion, bevel gear transmission is used, as shown in the cross section of the wrist mechanism in Fig. 2(b).

There were three design requirements for the bevel gear pairs: 1) The gear mechanism should be integrated into a tube with a diameter of 5 mm, 2) Large diameter for ease of machining and higher torque delivery and 3) ± 90 degrees in the pitch motion. For the bevel gear pairs, given the fixed size of the input gear, the diameter of the output gear that can fit into the 5 mm cylinder is larger when the angle between the axis Σ , is larger than 90 degrees. Thus, the bevel gear pairs with the oblique axis can exert larger torque compared to the pair with the perpendicular axis. To determine the angle between the two axes of the gears, we consider the following geometry of the mechanism

The range of the articulating motion of the wrist mechanism depends on its geometry. When a tool initially oriented along a unit vector \vec{v}_0 is oriented to $\vec{v} = [\sin \phi \cos \theta, \sin \phi \sin \theta, \cos \phi]$ in spherical coordinate by combining rotations about two non-parallel axes $\vec{\omega}_1$ and $\vec{\omega}_2$ intersecting at a common point, as shown in Fig. 3, the range of the polar angle ϕ and the azimuth angle θ will depend on the relative angles among $\vec{\omega}_1$, $\vec{\omega}_2$ and \vec{v}_0 . In laparoscopic instruments, $\vec{\omega}_1$ and \vec{v}_0 needs to be aligned with the major axis of the instrument shaft so that the instrument is straight at the initial configuration. In this case, mathematical analysis shows that the range of the θ is $[0, 2\pi]$ and the range of the ϕ is $[0, 2\beta]$ where the β is an angle between $\vec{\omega}_1$ (or \vec{v}_0) and $\vec{\omega}_2$.

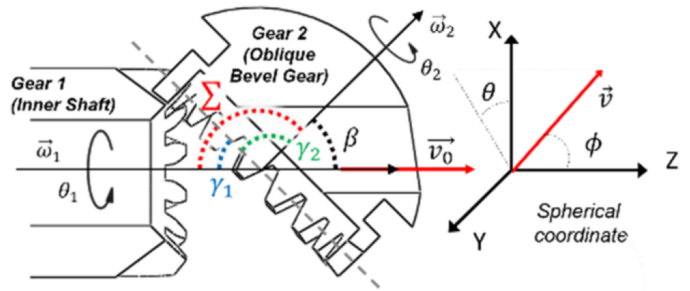


Fig. 3. Kinematics of the wrist and bevel gear design parameters.

The design goal for the articulating motion range was to span the front half sphere of the tool, which corresponds to $\phi \in [0^\circ, 90^\circ]$, and hence, β should be 45 degrees. Due to the constraint in oblique bevel gear design described in the next paragraph, in the actual design, β is 45.1 degrees.

As shown in Fig. 3, when bevel gears transmit motion between two non-parallel axes separated by angle Σ , pitch angles γ_1, γ_2 and the number of teeth n_1, n_2 of the gear pairs are related as below.

$$\gamma_2 = \Sigma - \gamma_1 = \arctan \left[\frac{\sin \Sigma}{\frac{n_1}{n_2} + \cos \Sigma} \right] \quad (1)$$

In our design, γ_2 was set to 90 degrees, so that the gear 2 (oblique bevel gear) takes the form of the crown gear whose teeth profile is easier to be machined than the other bevel gears with different pitch angle. This requires

$$\frac{n_1}{n_2} + \cos \Sigma = 0 \quad (2)$$

The integer pair $n_1 = 12$ and $n_2 = 17$ gives shaft angle Σ

$$\Sigma = -\arccos \frac{n_1}{n_2} = -\arccos \frac{12}{17} = 134.9^\circ \quad (3)$$

Then the pitch angle of the gear 1 (inner shaft) is 44.9 degrees and the angle β between \vec{v}_0 and $\vec{\omega}_2$ is 45.1°. This results in the range of the azimuthal angle ϕ is $[0^\circ, 90.2^\circ]$ which is close to the design goal of $\phi \in [0^\circ, 90^\circ]$.

Given pitch angle and teeth number, detailed teeth profile of the oblique bevel gear pair was designed following the standard defined in [45], and machined from stainless steel using 5 axis CNC. Then, one of the oblique gear pair was assembled to the inner shaft and the other was assembled to a casing made of PEEK (Polyether ether ketone), yellow part in Fig. 4(b), which is connected to the outer shaft. The yellow casing holds the position of the oblique gear and works as a bearing for rotational movement of the oblique gear.

B. Spring Loaded Graspers

Various tools can be attached to the wrists such as graspers, electrocautery, scissors, and a CMOS camera. In this letter, a grasper was selected as an exemplary tool. Due to the high design efforts and manufacturing costs for building a 5 mm diameter grasper from scratch, existing graspers from a common 5 mm straight laparoscopic instruments were modified.

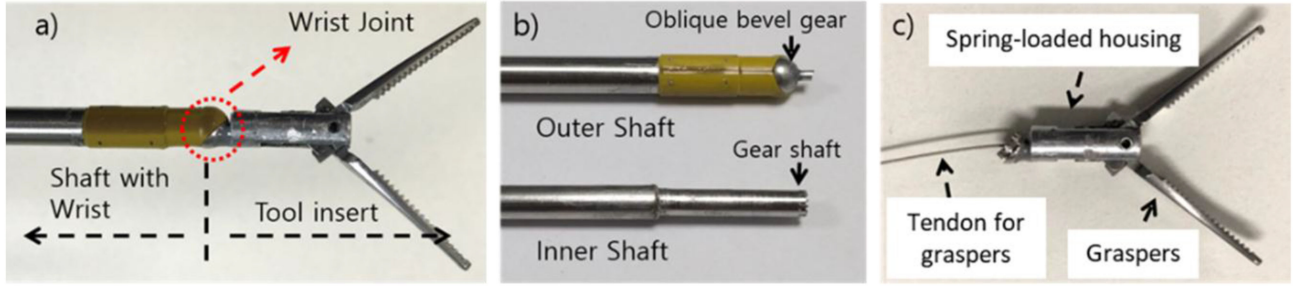


Fig. 4. (a) 5 mm dexterous micro-laparoscopic instruments (b) the inner and outer shaft with wrists, and c) the spring-loaded graspers.

Graspers of straight laparoscopic instruments without wrists use the rigid push-pull rod to actuate slider and crank mechanism that opens and closes the grasper. However, the rigid push-pull rod cannot be used for the graspers articulated by the wrist. In order to actuate the grasper even when the grasper is rotated by the wrist, push/pull rod is replaced by a tendon. Tendon can transmit pulling force to the grasper to close it even when the wrist is bent, but it cannot apply push force for opening the grasper. Therefore, the slider-crank mechanism of the grasper was assembled to the spring-loaded housing as shown in Fig. 2(c). Spring is compressed when the tendon is pulled to close the grasper and provides a restoring force that opens the grasper when the tension on the tendon is released.

Fig. 4(c) shows the actual grasper. The grasper and slider crank mechanism were disassembled from a commercial 5 mm laparoscopic tool (101.049A, Hangzhou Kangji Medical Instruments, China), the push-pull rod of the mechanism was replaced by a tendon and were assembled into a spring-loaded housing. Since the tendon will be subject to repeated sharp bending during the articulating wrist motion, 0.3 mm Dyneema rope (Dyneema, USA), which is capable of sharp bending without kink, is used as the tendon. The housing is assembled to the bevel gear by small connection tube that is welded on both gear and the housing.

C. Kinematic Analysis

The rotation of the inner and outer shafts, j_1 and j_2 , rotates the attached grasper about two axes $\vec{\omega}_1$ and $\vec{\omega}_2$ by θ_1 and θ_2 . Since $\vec{\omega}_1$ is aligned with the axes of the outer shaft.

$$\theta_1 = j_1 \quad (4)$$

The oblique bevel gear is driven by inner shaft while it is mounted on the casing that rotates together with the outer shaft. Inner, outer shafts and the bevel gear form a differential gear system. As a result, the rotation angle θ_2 of the oblique bevel gear is proportional to the difference between j_1 and j_2 , multiplied by gear ratio between the inner shaft and the oblique bevel gear.

$$\theta_2 = (j_2 - j_1) * \frac{12}{17} \quad (5)$$

As shown in Fig. 3, end effector initially oriented along \vec{v}_0 changes its direction to \vec{v} in spherical coordinates $[\phi, \theta]$ by rotating about $\vec{\omega}_1$ by θ_1 and then rotating about $\vec{\omega}_2$ by θ_2 .

$$\vec{v} = [\sin \phi \cos \theta, \sin \phi \sin \theta, \cos \phi]^T = e^{\hat{\omega}_1 \theta_1} e^{\hat{\omega}_2 \theta_2} \vec{v}_0 \quad (6)$$

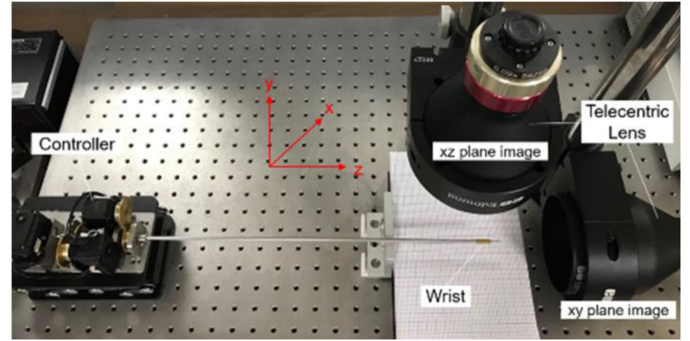


Fig. 5. Tip direction control experiment of the wrist.

where $\vec{\omega}_1 = [0, 0, 1]^T$, $\vec{\omega}_2 = [\cos 45.1^\circ, 0, \sin 45.1^\circ]^T$ and $\vec{v}_0 = [0, 0, 1]^T$. Inverse kinematics problem in (6) is well known Paden-Kahan Subproblem [46] which has analytic solutions for $[\theta_1, \theta_2]$. Then from $[\theta_1, \theta_2]$ desired motor shaft rotations $[j_1, j_2]$ can be calculated from (4) and (5).

III. EXPERIMENTS

A. Experimental Results of the Tip Direction Control

The accuracy of the articulating motion by the wrist was evaluated by comparing the commanded and measured the direction of the tip oriented by the wrist. The controller is set up to control the rotation of inner and outer shafts by rotational motors (Dynamixel 28AT, Robotis, South Korea). Also, there is an additional motor to pull wire for folding the graspers or other end effectors. The rotational motors are able to control the rotation angle by 0.0879 degrees per single motor step and 63 rpm.

Two telecentric lenses (0.09X 1/2" GoldTL Telecentric Lens, Edmund Optics, NJ, USA) with a monochrome image sensor (EO-1312M, Edmund Optics, NJ, USA) were installed to take an image of the tip at xz and xy plane, respectively. The monochrome image sensor is suitable for high resolution of the enlarged image. From the images of xz and xy plane, we measured the tip's direction about z axis and x axis, respectively, as Fig. 5. As illustrated in Fig. 6, let α be the angle between z-axis and the tip in xz plane, and let β be the angle between the x-axis and the tip in xy plane. From the measured angles, α and β , the unit vector of the tip direction, $\vec{V}_{\text{tip, exp}}$, is

TABLE I
COMPARISON OF THE TIP DIRECTION BETWEEN THEORETICAL AND EXPERIMENTAL RESULTS IN SPHERICAL COORDINATES

#	$\vec{V}_{tip,theo}$ (deg)	$\vec{V}_{tip,exp}$ (deg)	$ \theta_{diff} $ (deg)	#	$\vec{V}_{tip,theo}$ (deg)	$\vec{V}_{tip,exp}$ (deg)	$ \theta_{diff} $ (deg)	#	$\vec{V}_{tip,theo}$ (deg)	$\vec{V}_{tip,exp}$ (deg)	$ \theta_{diff} $ (deg)
	(ϕ, θ)	(ϕ, θ)			(ϕ, θ)	(ϕ, θ)			(ϕ, θ)	(ϕ, θ)	
1	5, 0	5.1, 0.3	0.07	11	25, 240	25.6, 117.8	1.12	21	65, 120	65.2, 57.6	2.18
2	5, 60	5.0, 60.2	0.04	12	25, 300	24.5, 62.2	1.05	22	65, 180	66.7, 178.9	1.98
3	5, 120	4.7, 121.3	0.29	13	45, 0	44.8, 0.5	0.41	23	65, 240	64.3, 237.0	2.81
4	5, 180	5.1, 178.9	0.14	14	45, 60	45.7, 61.9	1.54	24	65, 300	64.1, 298.3	1.79
5	5, 240	4.7, 121.0	0.30	15	45, 120	45.5, 57.6	1.78	25	85, 0	85.7, 0.6	0.92
6	5, 300	5.1, 60.7	0.15	16	45, 180	43.2, 179.3	1.86	26	85, 60	84.8, 60.5	0.52
7	25, 0	26.3, 0.6	1.33	17	45, 240	42.5, 117.7	2.93	27	85, 120	85.4, 121.7	1.74
8	25, 60	23.8, 59.2	1.29	18	45, 300	45.0, 61.8	1.27	28	85, 180	84.8, 179.4	0.63
9	25, 120	26.4, 121.7	1.55	19	65, 0	66.9, 0.8	2.04	29	85, 240	85.9, 237.8	2.36
10	25, 180	4.5, 178.8	0.71	20	65, 60	67.1, 61.0	2.27	30	85, 300	86.0, 298.0	2.25

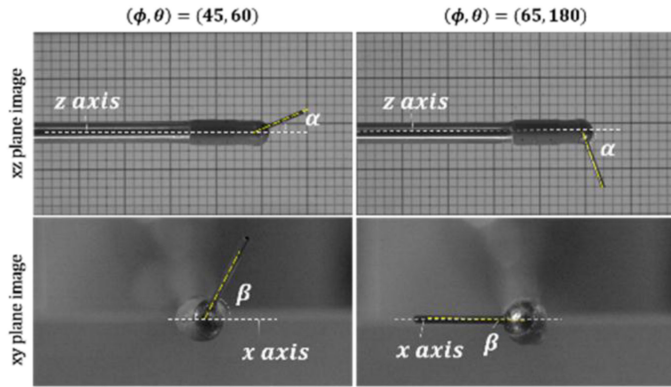


Fig. 6. The direction of tip from xz plane and xy plane in the tip control experiment.

calculated as (7).

$$\vec{V}_{tip,exp} = \frac{(\sin \alpha, \sin \alpha \tan \beta, \cos \alpha)}{\sqrt{1 + \sin^2 \alpha \tan^2 \beta}} \quad (7)$$

The theoretical unit vector of the tip direction (ϕ, θ) in spherical coordinate is converted into (8) in Cartesian coordinates.

$$\vec{V}_{tip,theo} = (\sin \phi \cos \theta, \sin \phi \sin \theta, \cos \phi) \quad (8)$$

The difference angle between theoretical and experimental direction, $\vec{V}_{tip,exp}$ and $\vec{V}_{tip,theo}$, is determined by (9).

$$\theta_{diff} = \arccos(\vec{V}_{tip,exp} \cdot \vec{V}_{tip,theo}) \quad (9)$$

Using the motorized system, we performed the tip control experiment for $\phi \in \{5^\circ, 25^\circ, 45^\circ, 65^\circ, 85^\circ\}$ and $\theta \in \{0^\circ, 60^\circ, 120^\circ, 180^\circ, 240^\circ, 300^\circ\}$ in spherical coordinate, summing up thirty cases in total. The experimental results were compared to the theoretical ones in Table I for the thirty cases; the average difference is 1.31° , and its standard deviation is 0.85° . Thanks to its gear-based mechanism, the suggested wrist demonstrated precise and consistent manipulation results compared to other mechanisms based on the bending of compliant

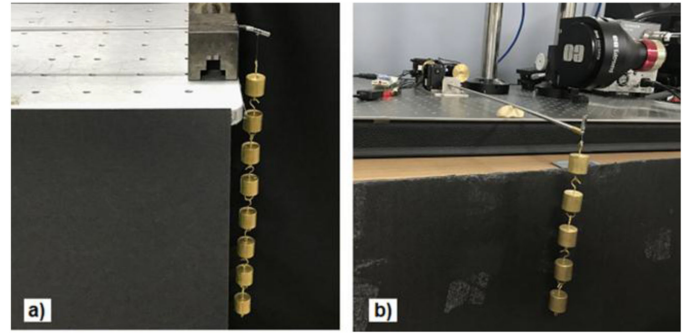


Fig. 7. Load capacity experiment setup. (a) The wrist structure endures 400 g of static load. (b) The wrist can be manipulated up to 250 g load at maximum while moving from $(0^\circ, 0^\circ)$ to $(90^\circ, 90^\circ)$ in the spherical coordinate.

materials or tendon-pulley mechanism. The experimental error could be minimized through exactly perpendicular alignment among the lens and the tip to have the exact image on the xy and xz plane. Additionally, the supplementary video demonstrates the sharp articulating motion and dexterity of the wrist. With 63 rpm speed of the rotational motors, the tip direction can be promptly controlled. different environments. The supplementary video demonstrates how the robotic system relocates the objects during the pick and place test.

In the peg test, using the teleoperated control system, one controlled the stylus to move five objects consecutively to the opposite side of the pegboard. The one monitored the enlarged view of the pegboard and end-effectors during teleoperation like Fig. 8(c). The one was trained to use the teleoperated control system for twenty minutes before the test. Timing for this task began when the graspers touched the first object, and the timing ends upon release of the last object. The test was performed for ten times and the average time was 98.7 seconds with the standard deviation of 6.37 seconds. The supplementary video demonstrates the peg transfer test with the proposed robotic system.

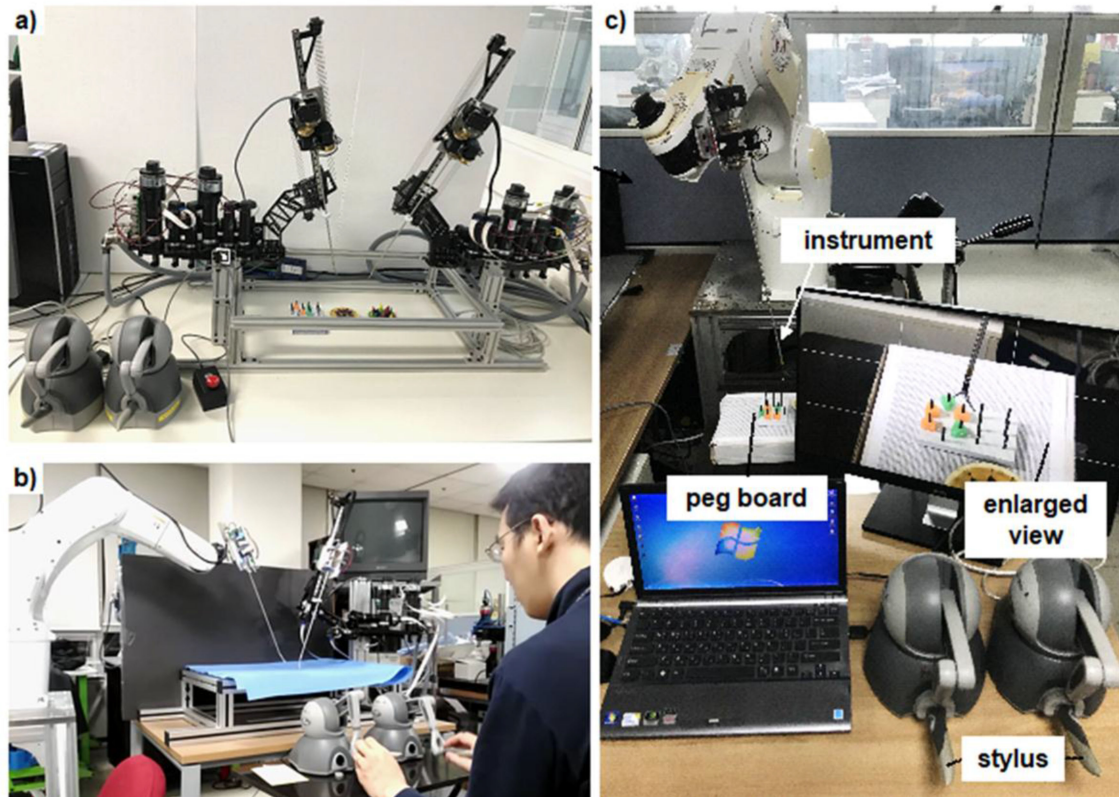


Fig. 8. (a) the bimanual teleoperated system with Raven II robot arms, (b) using the master/slave control system, the user controls the movement of the instrument, (c) the teleoperated control system for the peg transfer test. The user can monitor the enlarged view of the peg board and the instrument in real time while manipulating the stylus to control the movement of the instrument. During the test, the user moves the five objects consecutively to the opposite side of the peg board.

B. Load Capacity Test on the Wrist

The load test was performed to examine how much force it exerts with the suggested wrist and how much force the wrist endures. The stainless steel oblique bevel gear is welded with the housing part of an end effector of stainless steel. In the first test, a wire was fixed to the housing part through a hole 12 mm from the joint, as shown in Fig. 4(c), and then the wire was loaded. As Fig. 7(a), the wrist endures 400 g of the load.

Secondly, when a load was applied to the wire, the wrist's direction was manipulated from $(0^\circ, 0^\circ)$ to $(90^\circ, 90^\circ)$ in the spherical coordinate. The test examined whether the wrist moved exactly to $(90^\circ, 90^\circ)$ direction under the load. At maximum, the wrist was manipulated to the desired direction under 250 g of the load as in Fig. 7(b).

Thus, the wrist shows 400 g load capacity at static state, while 250 g load capacity at a dynamic state. In both tests, the failure occurred at the shaft that connects the oblique bevel gear to the housing of an end effector of Fig. 4(c). Increasing the thickness of the shafts can raise both the rigidity and load capacity of the wrist structure. The thickness can be optimized in the consideration of the dimension of the whole structure and additional tool that passes through the hollow passage. With advanced micromanufacturing technology, the oblique bevel gear part and the housing part can be made into one structure to enhance its rigidity. Also, the wrist load capacity can be

increased by replacing stainless steel components with more rigid materials such as titanium or titanium alloy.

C. Peg Transfer Test With the Teleoperated Control System

The wrist system was integrated to 6-axis robot arms to create the bimanual teleoperated surgical robot system. The kinematics of the wrist mechanism was solved and a motorized driver that controls two DoF wrist and the additional DoF for the graspers was built. Two robotic instruments were attached to 6-DoF RAVEN-II robot arm [47] or Denso VS065 robot arm (Denso Robotics, CA, United States) [48], and Sensable Phantom Omni haptic device (3D Systems, SC, USA) to build the master/slave control system as illustrated in Fig. 8(a) and (b).

The system enables the bimanual teleoperated control of the wrist. An operator grasps the stylus of Phantom Omni with each hand, the direction of each stylus is synchronized with the wrist's tip direction, and the movement of each stylus is synchronized with the movement of each robot arm in real-time. The operator can also fold/unfold the graspers by pressing the button of the stylus to pull/loosen the wire. The feasibility of the robotic instrument was verified by pick and place experiment for various objects and peg transfer test. The goal of the pick and place test was to move a wide range of objects, from 0.5 to 30 mm in diameter, from one column to another in different environments. The supplementary video demonstrates

how the robotic system relocates the objects during the pick and place test.

In the peg test, using the teleoperated control system, one controlled the stylus to move five objects consecutively to the opposite side of the pegboard. The one monitored the enlarged view of the pegboard and end-effectors during teleoperation like Fig. 8(c). The one was trained to use the teleoperated control system for twenty minutes before the test. Timing for this task began when the graspers touched the first object, and the timing ends upon release of the last object. The test was performed for ten times and the average time was 98.7 seconds with the standard deviation of 6.37 seconds. The supplementary video demonstrates the peg transfer test with the proposed robotic system.

IV. CONCLUSION

A 5 mm micro-laparoscopic instrument with new wrist mechanism is presented. The wrist mechanism converts the rotation of two concentric shafts into the sharp articulating motion of the wrist through the oblique bevel gear. End effectors can be oriented to any directions in the front hemisphere of the instrument tip. Use of concentric shafts provides advantages scalability both in terms of manufacturing and assembly. Gear transmission provides higher accuracy compared to the tendon pulley transmission used in the wristed laparoscopic instruments and thus may have advantages as an end effector for recently emerging researches in autonomous surgical robots.

Motorized driver system that actuates the developed instrument by rotating the concentric shafts were built. The robotic wrist system was evaluated in terms of dexterity, and rigidity. The wrist mechanism demonstrated tip orienting accuracy of 1.31° on average error, endured 400 g load at static state, and manipulated 250 g load at dynamic state. For comparison, consider a tendon-pulley mechanism using a pulley with 4 mm diameter. Rotation of the pulley by 1.31° corresponds to tendon displacement of $2\pi \cdot 1.31/180.0 = 46 \mu\text{m}$. Considering the deformation of tendons, it is not easy to get 1.31° tip orienting accuracy error with tendon-pulley mechanism.

Feasibility of the instrument was verified through pick and place experiment and peg transfer test using a teleoperated surgical robot equipped with the instrument. The peg transfer for five ring objects took 98.7 seconds on average with our gripper. According to Fundamentals of Laparoscopic Surgery (FLS) Program by Society of American Gastrointestinal and Endoscopic Surgeons [49], the peg transfer test should be done in 300 seconds for six ring objects with two grippers. Therefore, even if it is not the exactly same situation, the proposed robot is likely to meet the FLS program standard.

Although the feasibility of the laparoscopic instrument using oblique bevel gear wrist mechanism was demonstrated, there exists plenty of room for improvements before the instrument can be tested in real surgery situations.

As for the wrist mechanism, there exist two limitations. First, since the wrist mechanism provides roll and pitch degrees of freedom (DoF), the mechanism becomes singular when the attached tool is aligned with the roll axis. This can cause large

changes in the commanded joint angle when the commanded tool orientation passes the singular configuration. Secondly, due to the fact that the pitch motion of the tool is generated by the combined rotation of two axes, when the wrist makes pure pitch motion, the tool rotates about its major axis. This can cause out of the plane motion of a grasped object during pitch motion, which will be undesirable in suture tasks. Both limitations can be observed in the supplementary video.

In future works, 3rd DoF will be added to the mechanism to solve either one of the aforementioned limitations. If yaw axis rotation is added as a 3rd DoF, the lost degree of freedom at the singular configuration can be recovered. On the other hand, if roll axis rotation is added, the rotation of the tool during pitch motion can be compensated. Our initial experience shows that using torque coils delivered through the central lumen can transfer rotations to the attached tools even when the wrist is articulated and can be used to add 3rd roll DoF. create roll axis roll axis rotation can be added.

Finally, the assembly of the housing will be reinforced to improve the load capacity. Also, the sealing of the wrist mechanism will be investigated to protect the gear mechanism from the contact with the biological fluid.

As for the tool inserts, slider crank mechanism driving the grasper increases the length of the tool inserts and offsets the grasper from the wrist. This limited the precise movement of the tooltip and increased the motion envelop size of the instrument. In future research, we plan to bring graspers closer to the wrist by optimizing the link lengths of the slider-crank mechanism, or by using alternate mechanisms for driving the graspers. Finally, another tool inserts, such as CMOS image sensors will be attached to use as a steerable laparoscope that will allow surgeons to look around the tight corners.

REFERENCES

- [1] N. Patel *et al.*, "Evaluation of a novel flexible snake robot for endoluminal surgery," *Surg. Endosc.*, vol. 29, no. 11, pp. 3349–3355, 2015.
- [2] H. M. Le, T. N. Do, and S. J. Phee, "A survey on actuators-driven surgical robots," *Sens. Actuators A, Phys.*, vol. 247, pp. 323–354, 2016.
- [3] V. Vitiello, S.-L. Lee, T. P. Cundy, and G.-Z. Yang, "Emerging robotic platforms for minimally invasive surgery," *IEEE Rev. Biomed. Eng.*, vol. 6, pp. 111–126, 2013.
- [4] C. A. Seneci *et al.*, "Design and evaluation of a novel flexible robot for transluminal and endoluminal surgery," in *Proc. Int. Conf. IEEE/RSJ Intell. Robots Syst.*, 2014, pp. 1314–1321.
- [5] P. Breedveld, H. G. Stassen, D. W. Meijer, and J. J. Jakimowicz, "Manipulation in laparoscopic surgery: Overview of impeding effects and supporting aids," *J. Laparoendosc. Adv. Surg. Tech.*, vol. 9, no. 6, pp. 469–480, Dec. 1999.
- [6] T. G. Cooper, D. T. Wallace, S. Chang, S. C. Anderson, D. Williams, and S. Manzo, "Surgical tool having positively positionable tendon-actuated multi-disk wrist joint," US 6 817 974B2, Nov. 16, 2004.
- [7] G. S. Guthart and J. K. Salisbury, "The Intuitive/sup TM/ telesurgery system: Overview and application," in *Proc. Millennium Int. Conf. IEEE Robot. Autom.*, 2000, vol. 1, pp. 618–621.
- [8] T. L. Nguyen, T. N. Do, M. W. S. Lau, and S. J. Phee, "Modelling, design, and control of a robotic running foot for footwear testing with flexible actuator," in *Proc. 1st Int. Conf. Sports Sci. Technol.*, 2014, pp. 505–514.
- [9] R. J. Webster and B. A. Jones, "Design and kinematic modeling of constant curvature continuum robots: A review," *Int. J. Robot. Res.*, vol. 29, no. 13, pp. 1661–1683, Nov. 2010.
- [10] N. Simaan *et al.*, "Design and integration of a telerobotic system for minimally invasive surgery of the throat," *Int. J. Robot. Res.*, vol. 28, no. 9, pp. 1134–1153, Sep. 2009.

- [11] J. Shang *et al.*, "Design of a multitasking robotic platform with flexible arms and articulated head for Minimally Invasive Surgery," in *Proc. Int. Conf. IEEE/RSJ Intell. Robots Syst.*, 2012, pp. 1988–1993.
- [12] M. de Volder, A. J. M. Moers, and D. Reynaerts, "Fabrication and control of miniature McKibben actuators," *Sens. Actuators A, Phys.*, vol. 166, no. 1, pp. 111–116, Mar. 2011.
- [13] A. de Greef, P. Lambert, and A. Delchambre, "Towards flexible medical instruments: Review of flexible fluidic actuators," *Precis. Eng.*, vol. 33, no. 4, pp. 311–321, Oct. 2009.
- [14] M. D. Volder and D. Reynaerts, "Pneumatic and hydraulic microactuators: A review," *J. Micromech. Microeng.*, vol. 20, no. 4, Mar. 2010, Art. no. 043001.
- [15] M. Cianchetti, T. Ranzani, G. Gerboni, I. D. Falco, C. Laschi, and A. Menciassi, "STIFF-FL0P surgical manipulator: Mechanical design and experimental characterization of the single module," in *Proc. Int. Conf. IEEE/RSJ Intell. Robots Syst.*, 2013, pp. 3576–3581.
- [16] G. Gerboni, T. Ranzani, A. Diodato, G. Ciuti, M. Cianchetti, and A. Menciassi, "Modular soft mechatronic manipulator for minimally invasive surgery (MIS): Overall architecture and development of a fully integrated soft module," *Meccanica*, vol. 50, no. 11, pp. 2865–2878, Nov. 2015.
- [17] B. C.-M. Chang, J. Berring, M. Venkataram, C. Menon, and M. Parameswaran, "Bending fluidic actuator for smart structures," *Smart Mater. Struct.*, vol. 20, no. 3, Feb. 2011, Art. no. 035012.
- [18] V. D. Sars, S. Haliyo, and J. Szewczyk, "A practical approach to the design and control of active endoscopes," *Mechatronics*, vol. 20, no. 2, pp. 251–264, Mar. 2010.
- [19] W. Makishi, T. Matunaga, Y. Haga, and M. Esashi, "Active bending electric endoscope using shape memory alloy coil actuators," in *Proc. 1st Int. Conf. IEEE/RAS-EMBS Biomed. Robot. Biomechatron.*, 2006, pp. 217–219.
- [20] K. Ikuta, M. Tsukamoto, and S. Hirose, "Shape memory alloy servo actuator system with electric resistance feedback and application for active endoscope," in *Proc. Int. Conf. IEEE Robot. Autom.*, 1988, vol. 1, pp. 427–430.
- [21] Y. Haga, M. Esashi, and S. Maeda, "Bending, torsional and extending active catheter assembled using electroplating," in *Proc. 13th Annu. Int. Conf. IEEE Micro Electro Mech. Syst.*, 2000, pp. 181–186.
- [22] J. K. Chang *et al.*, "Development of endovascular microtools," *J. Micromech. Microeng.*, vol. 12, no. 6, pp. 824–831, Nov. 2002.
- [23] M. Simi, R. Pickens, A. Menciassi, S. D. Herrell, and P. Valdastrì, "Fine tilt tuning of a laparoscopic camera by local magnetic actuation: Two-port nephrectomy experience on human cadavers," *Surg. Innov.*, vol. 20, no. 4, pp. 385–394, Aug. 2013.
- [24] L. Liu, S. Towfighian, and A. Hila, "A review of locomotion systems for capsule endoscopy," *IEEE Rev. Biomed. Eng.*, vol. 8, pp. 138–151, 2015, doi: [10.1109/RBME.2015.2451031](https://doi.org/10.1109/RBME.2015.2451031).
- [25] N. Garbin, C. di Natali, J. Buzzi, E. de Momi, and P. Valdastrì, "Laparoscopic tissue retractor based on local magnetic actuation," *J. Med. Devices*, vol. 9, no. 1, Mar. 2015, Art. no. 011005.
- [26] S. Park, K. Koo, S. M. Bang, J. Y. Park, S. Y. Song, and D. 'Dan' Cho, "A novel microactuator for micro biopsy in capsular endoscopes," *J. Micromech. Microeng.*, vol. 18, no. 2, Jan. 2008, Art. no. 025032.
- [27] H. Yamashita, K. Matsumiya, K. Masamune, H. Liao, T. Chiba, and T. Dohi, "Miniature bending manipulator for fetoscopic intrauterine laser therapy to treat twin-to-twin transfusion syndrome," *Surg. Endosc.*, vol. 22, no. 2, pp. 430–435, Feb. 2008.
- [28] V. Velanovich, "Laparoscopic vs open surgery," *Surg. Endosc.*, vol. 14, no. 1, pp. 16–21, Jan. 2000.
- [29] G. Gandaglia *et al.*, "Effect of minimally invasive surgery on the risk for surgical site infections: Results from the national surgical quality improvement program (NSQIP) database," *JAMA Surg.*, vol. 149, no. 10, pp. 1039–1044, Oct. 2014.
- [30] M. Braga *et al.*, "Laparoscopic versus open colorectal surgery: A randomized trial on short-term outcome," *Ann. Surg.*, vol. 236, no. 6, pp. 759–766, Dec. 2002.
- [31] F. Bagante *et al.*, "Minimally invasive vs. open hepatectomy: A comparative analysis of the national surgical quality improvement program database," *J. Gastrointest. Surg.*, vol. 20, no. 9, pp. 1608–1617, 2016.
- [32] L. Li, J. Tian, H. Tian, R. Sun, Q. Wang, and K. Yang, "The efficacy and safety of different kinds of laparoscopic cholecystectomy: A network meta analysis of 43 randomized controlled trials," *PLoS One*, vol. 9, no. 2, Feb. 2014, Art. no. e90313.
- [33] "BJ needle R," [Online]. Available: <http://www.nition.jp/products/?id=1452055714-050754>. [Accessed on: Sep. 4, 2018].
- [34] "Intuitive | da vinci surgical instruments | endowrist," *Intuitive Surg.*, [Online]. Available: <https://www.intuitive.com/en/products-and-services/davinci/instruments>. [Accessed on: Sep. 4, 2018].
- [35] MMI S.p.A., "MMI - Medical micro instruments," MMI S.p.A., Pisa, Italy, [Online]. Available: <http://www.mmimicro.com/>. [Accessed on: Sep. 4, 2018].
- [36] P. A. York, P. J. Swaney, H. B. Gilbert, and R. J. Webster, "A wrist for needle-sized surgical robots," in *Proc. Int. Conf. IEEE Robot. Autom.*, May 2015, vol. 2015, pp. 1776–1781.
- [37] "SILSTM hand instruments | medtronic," [Online]. Available: <http://www.medtronic.com/covidien/en-us/products/hand-instruments-ligation/sils-hand-instruments.html>. [Accessed on: Apr. 26, 2018].
- [38] J. Burgner-Kahrs, D. C. Rucker, and H. Choset, "Continuum robots for medical applications: A survey," *IEEE Trans. Robot.*, vol. 31, no. 6, pp. 1261–1280, Dec. 2015.
- [39] Y. Chen, J. Liang, and I. W. Hunter, "Modular continuum robotic endoscope design and path planning," in *Proc. Int. Conf. IEEE Robot. Autom.*, 2014, pp. 5393–5400.
- [40] P. E. Dupont, J. Lock, B. Itkowitz, and E. Butler, "Design and control of concentric-tube robots," *IEEE Trans. Robot.*, vol. 26, no. 2, pp. 209–225, Apr. 2010.
- [41] H. B. Gilbert, D. C. Rucker, and R. J. Webster III, "Concentric tube robots: The state of the art and future directions," in *Proc. 16th Int. Symp. Robot. Res.*, 2016, pp. 253–269.
- [42] S. M. Segreti, M. D. M. Kutzer, R. J. Murphy, and M. Armand, "Cable length estimation for a compliant surgical manipulator," in *Proc. Int. Conf. IEEE Robot. Autom.*, 2012, pp. 701–708.
- [43] T. Okubo *et al.*, "Hand-held multi-DOF robotic forceps for neurosurgery designed for dexterous manipulation in deep and narrow space," in *Proc. Annu. Int. Conf. IEEE Eng. Med. Biol. Soc.*, 2014, vol. 2014, pp. 6868–6871.
- [44] M. Fujii, K. Fukushima, N. Sugita, T. Ishimaru, T. Iwanaka, and M. Mitsuishi, "Design of intuitive user interface for multi-DOF forceps for laparoscopic surgery," in *Proc. Int. Conf. IEEE Robot. Autom.*, 2011, pp. 5743–5748.
- [45] ANSI/AGMA 2005-D03, *Design Manual for Bevel Gears*. Alexandria, VA, USA: AGMA, 2005.
- [46] B. E. Paden, "Kinematics and control of robot manipulators," Univ. California, Berkeley, CA, USA, Tech. Rep. UCB/ERL M86/5, 1986.
- [47] M. J. H. Lum *et al.*, "The RAVEN: Design and validation of a telesurgery system," *Int. J. Robot. Res.*, vol. 28, no. 9, pp. 1183–1197, Sep. 2009.
- [48] "VS-050/060 Series - Features - DENSO Robotics," [Online]. Available: <http://densorobotics.com/products/vs-050-060>. [Accessed on: Feb. 24, 2019].
- [49] FLS, "FLS program description," *Fundamentals of Laparoscopic Surgery*, Aug. 2010. [Online]. Available: <https://www.flsprogram.org/index/fls-program-description/>. [Accessed on: Jul. 02, 2019].